Electroacupuncture Facilitates the Integration of Neural Stem Cell-Derived Neural Network with Transected Rat Spinal Cord

Hui Jin,[1,8] Yu-Ting Zhang,[3,8] Yang Yang,[1] Lan-Yu Wen,[1] Jun-Hua Wang,[2] Hao-Yu Xu,[1] Bi-Qin Lai,[2] Bo Feng,[1] Ming-Tian Che,[1] Xue-Cheng Qiu,[1] Zhi-Ling Li,[4] Lai-Jian Wang,[5] Jing-Wen Ruan,[4] Bin Jiang,[5] Xiang Zeng,[2] Qing-Wen Deng,[2] Ge Li,[2] Ying Ding,[1,2,*] and Yuan-Shan Zeng[1,2,5,6,7,*]

[1]Key Laboratory for Stem Cells and Tissue Engineering, Ministry of Education, Sun Yat-sen University, Guangzhou 510080, China
[2]Department of Histology and Embryology, Zhongshan School of Medicine, Sun Yat-sen University, Guangzhou 510080, China
[3]Center of Reproductive Medicine of Shunde Hospital, Southern Medical University, Shunde, Guangdong 528300, China
[4]Department of Acupuncture, The First Affiliated Hospital, Sun Yat-sen University, Guangzhou 510080, China
[5]Guangdong Province Key Laboratory of Brain Function and Disease, Faculty of Forensic Medicine, Zhongshan School of Medicine, Sun Yat-sen University, Guangzhou 510080, China
[6]Co-innovation Center of Neuroregeneration, Nantong University, Nantong 226001, China
[7]Institute of Spinal Cord Injury, Sun Yat-sen University, Guangzhou 510120, China
[8]Co-first author
*Correspondence: dingying@mail.sysu.edu.cn (Y.D.), zengysh@mail.sysu.edu.cn (Y.-S.Z.)
https://doi.org/10.1016/j.stemcr.2018.12.015

SUMMARY

The hostile environment of an injured spinal cord makes it challenging to achieve higher viability in a grafted tissue-engineered neural network used to reconstruct the spinal cord circuit. Here, we investigate whether cell survival and synaptic transmission within an NT-3 and TRKC gene-overexpressing neural stem cell-derived neural network scaffold (NN) transplanted into transected spinal cord could be promoted by electroacupuncture (EA) through improving the microenvironment. Our results showed that EA facilitated the cell survival, neuronal differentiation, and synapse formation of a transplanted NN. Pseudorabies virus tracing demonstrated that EA strengthened synaptic integration of the transplanted NN with the host neural circuit. The combination therapy also promoted axonal regeneration, spinal conductivity, and functional recovery. The findings highlight EA as a potential and safe supplementary therapeutic strategy to reinforce the survival and synaptogenesis of a transplanted NN as a neuronal relay to bridge the two severed ends of an injured spinal cord.

INTRODUCTION

Spinal cord injury (SCI) disrupts the descending and ascending axonal tracts and this invariably results in loss of motor, sensory, and autonomic nerve functions below the lesion segments. In view of the complicated pathophysiological process of SCI, so far there is no effective treatment for SCI. To reverse the devastating outcomes caused by SCI, it is desirable as the first step to repair the damaged neuronal circuits for functional recovery.

In the past few decades, neural stem cell (NSC)-based therapies have been prominently featured in SCI neural regeneration (Yousefifard et al., 2016). Furthermore, the combinational application of biomaterials with NSCs is also being widely explored in the case of SCI (Agbay et al., 2016; Lin et al., 2016). It is known that neurotrophic factors modulate the proliferation, differentiation, and synaptogenesis of NSCs (Chao, 2003; Poo, 2001). We have reported earlier that the neurotrophin-3 (NT-3)/ TRKC signal pathway promotes the differentiation and synapse formation of NSC-derived neurons in vitro (Lai et al., 2016; Wang et al., 2007; Xiong et al., 2009). This was demonstrated by the fact that NT-3-overexpressed NSCs (NT-3 NSCs) could induce TRKC-overexpressed NSCs (TRKC NSCs) to differentiate into neurons with synaptic connections and the potency of synaptic transmis-

sion in a three-dimensional (3D) poly(lactide-co-glycolide) (PLGA) scaffold (Xiong et al., 2009). However, when this scaffold was transplanted into the transected spinal cord, only a small fraction of cells in the scaffold survived and most differentiated into astrocytes at the injury/graft site of the spinal cord (Du et al., 2011, 2014), which could be attributed to the absence of neurotrophic factors in the hostile microenvironment of the injured spinal cord (Bregman et al., 2002). To address the issue of the low survival rate of grafted cells, this study sought to use a feasible strategy to enhance the survival and neuronal differentiation of a grafted tissue-engineered neural network scaffold (NN).

Many studies, including ours, have reported that electroacupuncture (EA) treatment can effectively increase neurotrophic factor (such as NT-3, BDNF, etc.) secretion, inhibit inflammation, and promote axonal regeneration, synapse formation, and neural rehabilitation after SCI (Chen et al., 2015; Ding et al., 2009; Renfu et al., 2014). The EA treatment adopted by us is a model of electrical stimulation in the Governor Vessel (GV) acupoints, which are located in the sunken points between adjacent spinous processes at the midline level of the spine. Increasing studies have shown that electrical stimulation can guide the neurite growth in vitro and enhance neuron survival and locomotor function improvement of injured spinal cord in vivo (Han et al., 2016b; Hofstoetter et al., 2018; Yao and Li,
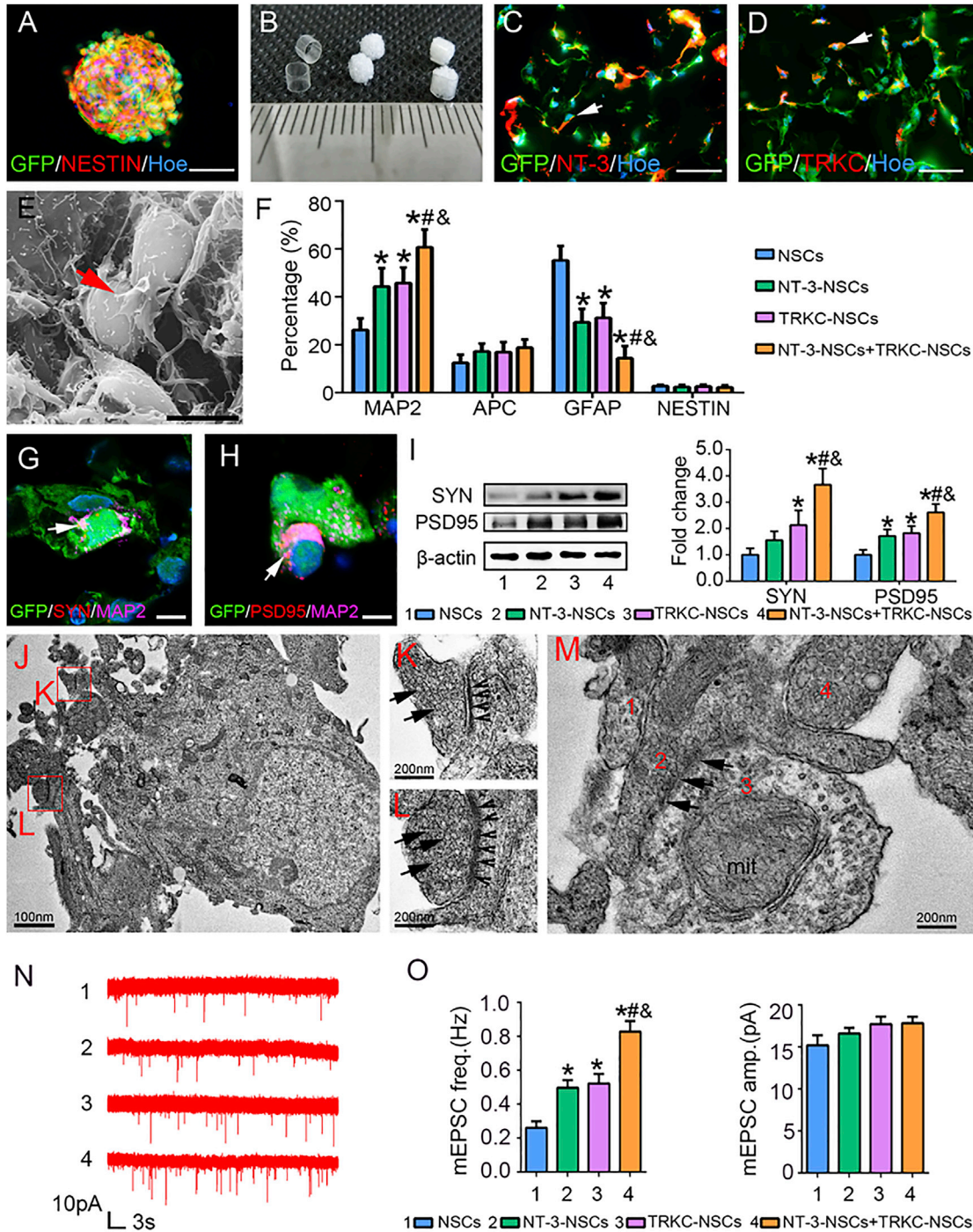
Figure 1. Co-culture of NT-3-NSCs and TRKC-NSCs in 3D GS *In Vitro* to Establish an NSC-Derived Neural Network Scaffold with Functional Synaptic Structure

(A) A neurosphere from GFP-transgenic rat pups comprised NESTIN[+] NSCs.

(B) PLGA tubes with diameter of 3 mm and length of 2 mm (left), a piece of GS (middle), and appearance of the GS scaffold (right).

(C) NSCs infected with Adv-NT-3 were NT-3^{+} staining (arrow).

(D) NSCs infected with Adv-TRKC showed TRKC[+] staining (arrow).

(E) Scanning electron microscopy showed that NSC-derived cells in the GS scaffold formed contacts with one another. A neurite of an NSC-derived neuron-like cell was in contact with another neuron-like cell body (red arrow).

2016; Zhang et al., 2017). However, a disadvantage of spinal electrical stimulation is the need for surgery and an implanted electrode array, which may have undesirable effects (Kumar et al., 2017). EA is widely used in clinical practice because of its effectiveness and safety for patients. Indeed, our previous study found that utilizing EA on GV acupoints enhances the survival and migration of transplanted NSCs in the injured spinal cord, but the grafted NSCs without gene modification or pre-differentiation showed low efficiency of neurogenesis of functional neurons for the reconstruction of neural circuitry in injured spinal cord (Chen et al., 2008). Here, the combination of NSC-derived NN transplantation and EA treatment is considered an ideal or optimal approach to achieving higher survival and neuronal differentiation of grafted NSCs.

In the present study we first *in vitro* co-cultured NT-3 NSCs and TRKC NSCs in a 3D gelatin sponge scaffold (GS) to establish an NSC-derived NN with synaptic transmission. The NN was then transplanted into the transected spinal cord to investigate whether, when coupled with EA application, the survival and synaptic transmission of the grafted NN could be promoted by enhancing the secretion of endogenous NT-3 in the injured spinal cord.

RESULTS

Co-culture of NT-3 NSCs and TRKC NSCs in 3D GS *In Vitro* to Establish an NSC-Derived Neural Network Scaffold with Functional Synaptic Structure

NSCs derived from the hippocampus of GFP transgenic rat pups were aggregated as free-floating neurospheres in *in vitro* culture and expressed NESTIN (a marker for neural precursors, Figure 1A). NSCs were transfected by recombinant adenovirus containing the NT-3 gene (Ad-NT-3) or the TRKC gene (Ad-TRKC) and then seeded in the 3D GS scaffold (Figure 1B). The expression of NT-3 (Figure 1C)

and TRKC (Figure 1D) proteins in the NSCs was detected by immunofluorescence (IF) staining *in vitro* after 14-day co-culture. Western blot analysis also showed that expression of NT-3 or TRKC was significantly up-regulated in Adv-NT-3- or Adv-TRKC-transfected NSCs (Figure S1A). Scanning electron microscopy showed that NSC-derived neuron-like cells with neurites formed contacts with one another in the NT-3 NSC + TRKC NSC group (Figure 1E). Further, IF staining showed that most NSCs differentiated into three major cell types, namely, MAP2$^+$ neurons, APC$^+$ oligodendrocytes, and GFAP$^+$ astrocytes, with occasional ones being NESTIN$^+$ NSCs (Figure S1B). Statistical analysis of the cell types showed that the NT-3 NSC + TRKC NSC group had the highest percentage of MAP2$^+$ neurons (60.71% ± 7.37%) and the lowest percentage of GFAP$^+$ astrocytes (14.37% ± 5.04%), compared with other groups, and the percentage of APC$^+$ oligodendrocytes and NESTIN$^+$ NSCs did not change much among the four groups (Figure 1F). These findings suggest that the high expression of both NT-3 and TRKC increases the differentiation of NSCs into neurons.

To determine whether NSC-derived neurons in the GS scaffold could develop synapses, IF staining, electron microscopy (EM), and whole-cell patch clamp were performed. In the NT-3 NSC + TRKC NSC group, synapsin I (SYN, a pre-synaptic marker) (Figure 1G) and post-synaptic density 95 (PSD95, a post-synaptic marker) (Figure 1H) were localized in MAP2$^+$ neurons in 14-day culture. Western blot analysis revealed that the expression of SYN or PSD95 was the highest in the NT-3 NSC + TRKC NSC group (Figure 1I). EM showed that NSC-derived neurons extended some long neurites, which connected with one another to form synaptic structures (Figure 1J). The synapses showed a pre-synaptic component, synaptic cleft, and post-synaptic membrane (Figures 1K and 1L). The terminals of some neurites contained a cluster of spherical or flattened agranular vesicles (Figure 1M), indicating that they were chemical synapses. Moreover, NSC-derived neurons in the NT-3

(F) Bar chart showing the percentages of MAP2$^+$, APC$^+$, GFAP$^+$, and NESTIN$^+$ cells in the NSCs, NT-3-NSCs, TRKC-NSCs, and NT-3-NSCs + TRKC-NSCs groups (n = 5/group).

(G and H) MAP2$^+$ (purple, arrows), GFP$^+$ (green) NSC-derived neurons were labeled with (G) SYN (red) and (H) PSD95 (red) in the NT-3-NSCs + TRKC-NSCs group.

(I) Western blot analysis of SYN and PSD95 (n = 5/group).

(J–L) Transmission electron microscopy showing profiles of some synaptic structures between the NSC-derived neurons in the NT-3-NSCs + TRKC-NSCs group. (K and L) High magnifications of two boxed areas in (J) showing pre-synaptic components with spherical agranular vesicles (arrows), post-synaptic membrane (arrowheads), and synaptic cleft.

(M) EM showed that several neurite terminals (numbered from 1 to 4) aggregate together to form axodendritic-like or axoaxonal-like synapses (arrows).

(N) Representative traces of mEPSCs.

(O) Bar charts showing the frequency and amplitude of mEPSCs in 4 groups (n = 10/group).

One-way ANOVA with least significant difference (LSD) t; *$p < 0.05$ indicates significant difference from the NSC group; #$p < 0.05$ indicates significant difference from the NT-3 NSCs; &$p < 0.05$ indicates significant difference from the TRKC NSC group. Scale bars: 40 μm in (A), (C), and (D); 10 μm in (E); 5 μm in (G) and (H); 100 nm in (J); 200 nm in (K–M).

NSC + TRKC NSC group also exhibited expression of more neurotransmitters, such as choline acetyltransferase, glutaminase, and glutamate decarboxylase 67, than other groups (Figures S2A and S2B). Electrophysiology evaluation was performed by whole-cell patch clamp to detect miniature excitatory post-synaptic currents (mEPSCs) and action potentials (APs) generated by NSC-derived neurons. Under a holing potential of −70 mV, NSC-derived neurons exhibited the mEPSCs (Figure 1N). The quantification analysis showed that the frequency of mEPSCs in the NT-3 NSC + TRKC NSC (0.83 ± 0.20 Hz) group was significantly higher than that in the GS (0.26 ± 0.12 Hz), GS + EA (0.50 ± 0.14 Hz), and NN (0.52 ± 0.18 Hz) groups, but there was no difference in the amplitude of mEPSCs in the four groups (Figure 1O). About 10% of NSC-derived neurons could be recorded with one or more consecutive APs in the NT-3 NSC + TRKC NSC group (Figure S2C). Taken together, these results suggest that overexpression of NT-3 and TRKC in the NN may facilitate synaptogenesis of NSC-derived neurons with capability of synaptic transmission *in vitro*.

Survival and Neuronal Differentiation of Transplanted NSC-Derived Neural Network *In Vivo*

To investigate whether EA could promote grafted GFP+ cell survival, the GFP+ number and volume in the NN were measured. At 8 weeks after transplantation, a few GFP+ cells were distributed in the graft site of the spinal cord in the NN group, but more GFP+ cells were observed in the graft site and some migrated into the caudal host tissue in the NN + EA group (Figures 2A and S3). The number and volume of GFP+ grafts in the NN + EA group were larger than those in the NN group (Figure 2B; p < 0.05). In addition, western blot analysis also showed that GFP expression in the NN + EA group was more than that in the NN group (Figure 2C).

To evaluate differentiation phenotypes of grafted GFP+ cells, IF staining and counting of three types of differentiated cells were performed at 8 weeks after transplantation (Figures 2D–2G). Quantitative analyses showed that the percentage of MAP2+GFP+ neurons in the NN + EA (33.58% ± 6.37%) group was higher than that in the NN (11.50% ± 4.38%) group (Figure 2D), whereas the percentage of APC+GFP+ oligodendrocytes does not show significant difference between the NN + EA group and the NN group (Figure 2E). The percentage of GFAP+GFP+ astrocytes in the NN + EA (45.10% ± 5.51%) group was lower than that in the NN (71.95% ± 7.54%) group (Figure 2F). NESTIN+GFP+ NSCs were not found in the NN and NN + EA groups.

Synaptic Maintenance between NSC-Derived Neurons and Synapse Formation between NSC-Derived Neurons and Host Neurons

To evaluate whether EA is beneficial in maintaining synaptic structure and establishing new synaptic connections of grafted NSC-derived neurons with host neurons at 8 weeks after transplantation, IF staining and western blot were carried out. The results of SYN/MAP2/GFP and PSD95/MAP2/GFP triple-labeled IF staining showed that grafted MAP2+GFP+ neurons expressed less SYN and PSD95 in the NN group than those in the NN + EA group (Figure 3A). Especially, in the NN + EA group, many graft-derived MAP2+ neurons emitted intense SYN staining in the injury/graft site (Figure 3A). Western blot analysis showed that the expression of SYN and PSD95 in the NN + EA group was significantly higher than that in the NN group (Figure 3B). In addition, the GFP/NF/SYN triple-labeled IF indicated the potential of synaptic formation between the graft-derived neurons and the host NF+ axons in the NN + EA group (Figures 3C and 3D). Immunoelectron microscopy (IEM) further demonstrated that grafted GFP+ neurons could form synapse-like contacts with one another in the graft site of spinal cord in the NN + EA group (Figure 3E). In addition, IEM also showed that grafted GFP+ cells formed synapse-like structures with host neurons (Figures 3F and 3G). Taken together, these results suggest that EA may facilitate maintaining synaptic structure and establishing new synaptic-like connections of grafted NSC-derived neurons with host neurons.

Pseudorabies Virus Tracing

To determine whether EA could promote the integration of grafted NSC-derived neurons with spinal cord neural circuit, pseudorabies virus (PRV) was injected into the sciatic nerve bilaterally for retrograde transsynaptic tracing. The numbers of PRV-labeled neurons in the T9 (2 mm rostral to the injury/graft site), T10 (injury/graft site), and T11 (2 mm caudal to the injury/graft site) spinal segments were enumerated (Figure 4A). In the T9 and T10 segments, the number of PRV-labeled neurons in the NN + EA group was significantly higher than that in the NN group, but PRV-labeled neurons were absent in the T9 and T10 segments of the GS and GS + EA groups (Figures 4B and 4C). In the T11 segment, the number of PRV-labeled neurons in the NN + EA (28.57 ± 1.40) group was significantly higher than that in the GS + EA (21.53 ± 1.99) and GS (19.37 ± 1.66) groups, and the number of PRV-labeled neurons in the NN (26.77 ± 1.91) group was higher than that in the GS group (Figure 4C). The results suggest that EA treatment can enhance the integration of grafted NN as neuronal relays with the host spinal cord neural circuit to transmit neural signals from the rostral region across the injury/graft site to the caudal region of injured spinal cord.

Axonal Regeneration

To quantify the number of regenerating axons in the injury/graft site of spinal cord, GAP43 and NF immunostaining was performed. The results showed that NN graft and/or EA could promote regrowth of the GAP43+ axons into the
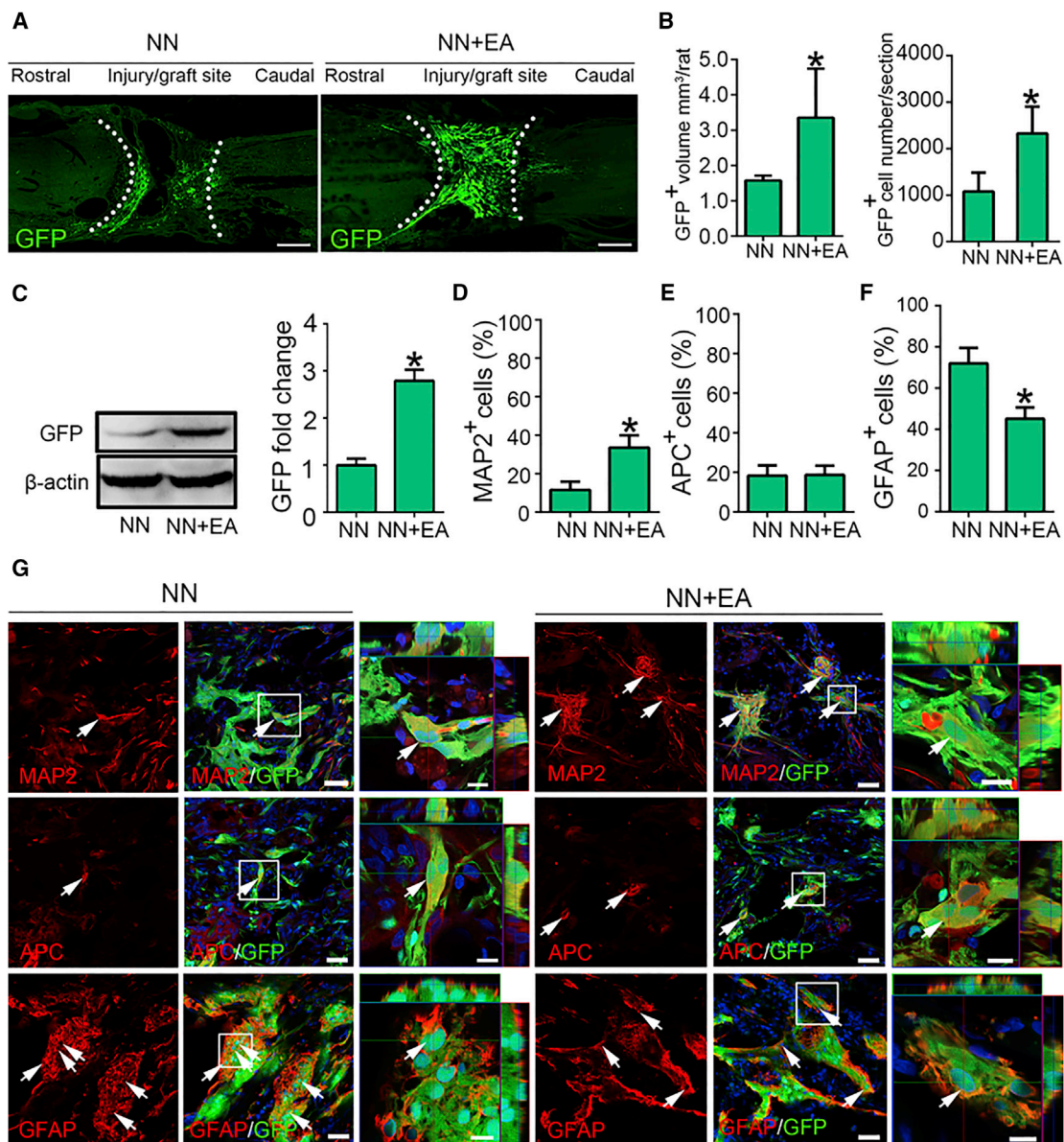
Figure 2. EA Promotes the Survival and Differentiation of NSC-derived Neurons in Transplanted Neural Network Scaffold *In Vivo*

(A) Representative confocal microscopy images from the NN and NN + EA groups 8 weeks after SCI. The dashed curves outline the interface of graft and host.

(B) Bar chart showing the quantification of the number and volume of grafted GFP+ cells (n = 5/group; Mann-Whitney U test, *p < 0.05).

(C) Western blot analysis of GFP expression in the injury/graft site in the NN + EA and NN groups at 8 weeks after SCI (n = 5/group; Student's t test, *p < 0.05).

(D–F) Bar charts showing the percentage of GFP+ cells differentiating into (D) MAP2+ neurons, (E) APC+ oligodendrocytes, and (F) GFAP+ astrocytes at 8 weeks after graft (n = 5/group; Student's t test, *p < 0.05).

(G) Representative confocal microscopy images for MAP2, APC, and GFAP IF (arrows).

Scale bars: 1 mm in (A); 40 μm in (G); 10 μm in the high-magnification boxed areas in (G).

injured site. Compared with the GS group, the relative density of GAP43+ axons was significantly increased in the areas rostral and caudal to the injury/graft site in the NN + EA, NN, and GS + EA groups (Figures 5A–5E). However, there was no significant difference in GAP43-positive axon relative density in the areas rostral and caudal to the injury/graft site between the GS + EA group and the NN group (Figures 5B, 5C, and 5E). In the NN + EA group, GAP43+ axon relative
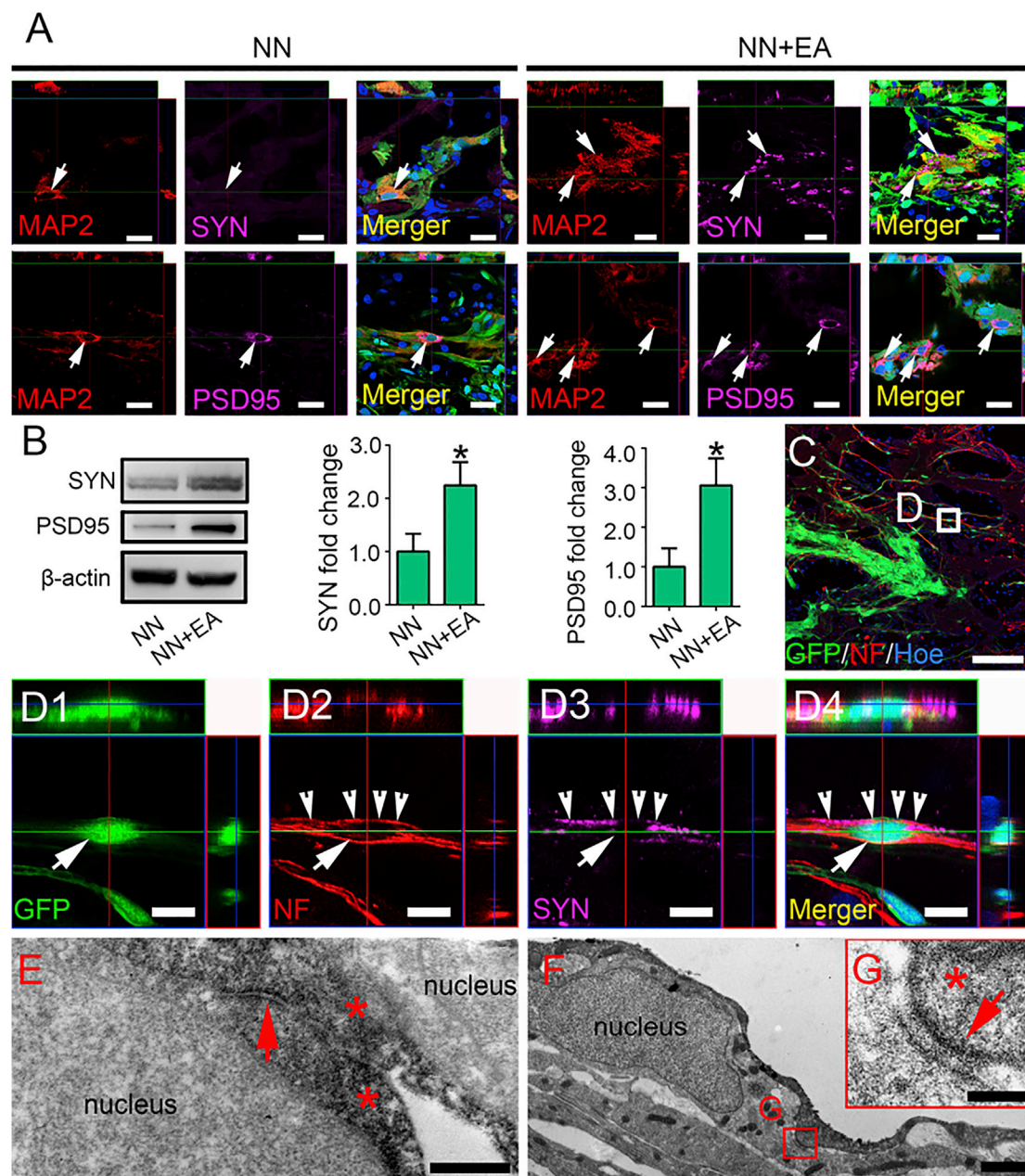
Figure 3. Maintenance and Establishment of Synaptic Connections in the Injury/Graft Site of Spinal Cord

(A) Representative images of cells triple labeled with GFP (green), MAP2 (red), and SYN (purple) or PSD95 (purple) in the epicenter of the injury/graft site. The merged images show the colocalization of GFP/MAP2/SYN or PSD95 (arrows).

(B) Western blot analysis of SYN and PSD95 expression in the graft site of spinal cord at 8 weeks after SCI (n = 5/group, Student's t test, *p < 0.05).

(C and D) (C) NF[+] host-derived axons and grafted GFP^{+} neurons in the injury/graft site of spinal cord were visualized by IF. (D1–D4) Magnified images of boxed area D in (C) that were triple labeled with (D1) anti-GFP (green), (D2) NF (red), (D3) SYN (purple), and (D4) their merged image. Arrow indicates a NF[+]GFP[+] cell in contact with a NF[+]SYN[+] host axon (arrowheads).

(E) Representative IEM image of grafted GFP^{+} cells (*, labeled by DAB) in the NN + EA group. The red arrow indicates a grafted GFP[+] cell (*) forming a synaptic contact with another GFP[+] cell (*).

(F) IEM image showing a host neuron and a GFP[+] (* in G) grafted cell process.

(G) An enlarged view of boxed area in (F) showing a synaptic-like contact (arrow).

Scale bars: 20 μm in (A) and (C); 10 μm in (D1)–(D4); 400 nm in (E); 1 μm in (F); 200 nm in (G).
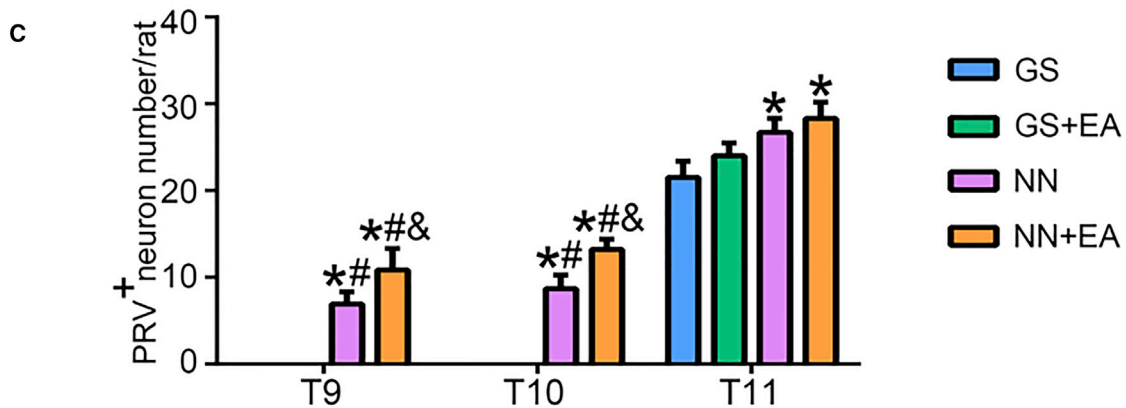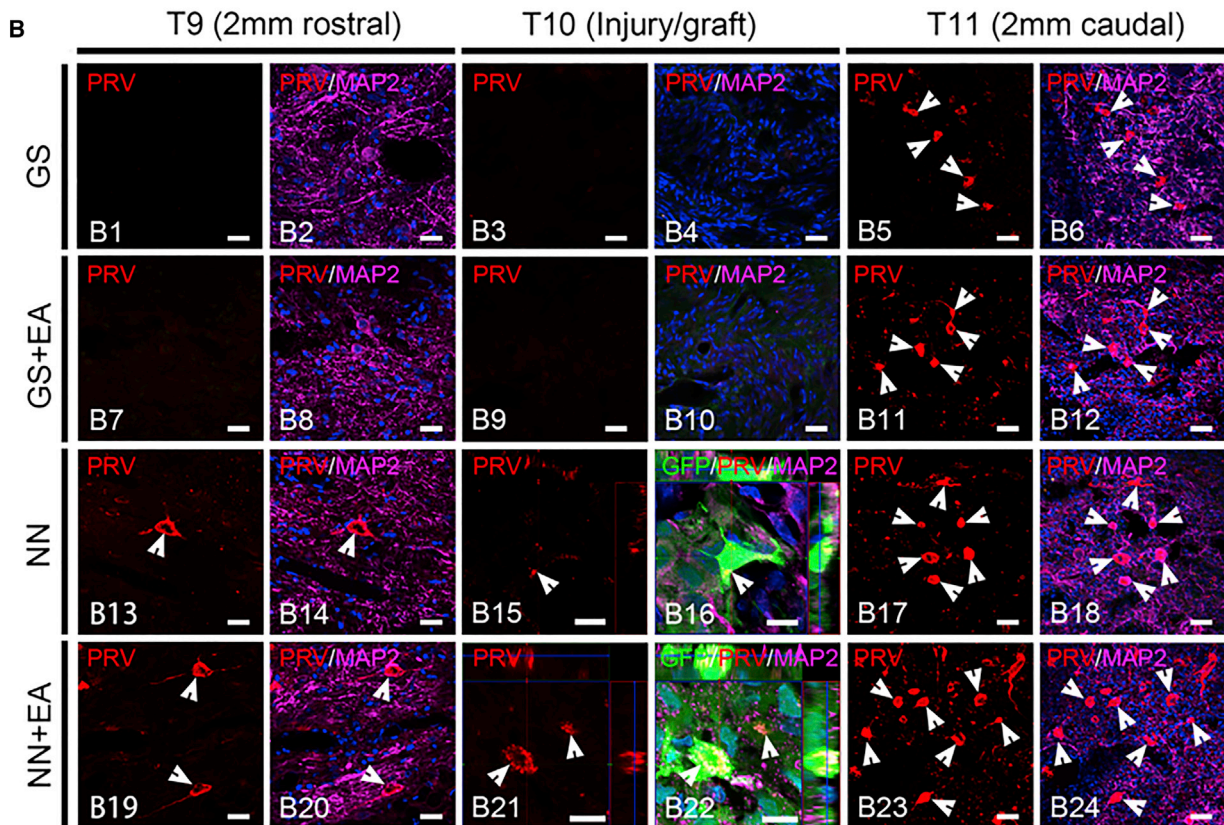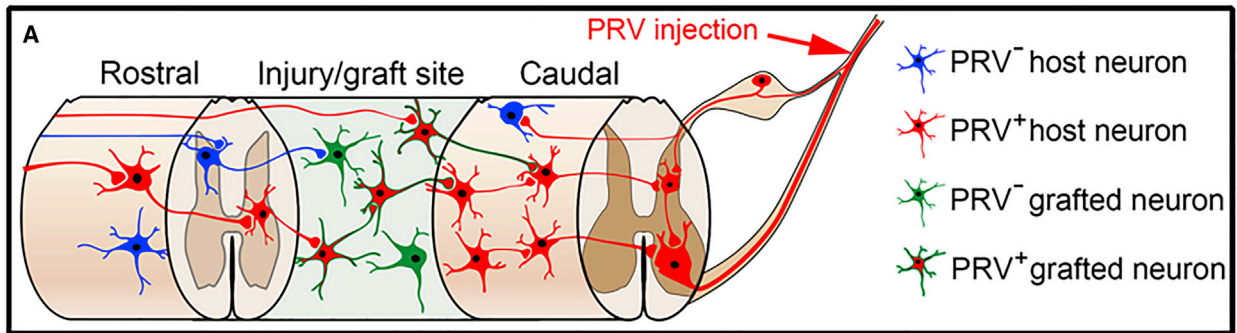
(legend on next page)

density in three areas was significantly higher than that in the GS, GS + EA, and NN groups (Figures 5A–5E). Furthermore, the results of NF immunostaining were comparable to those of GAP43. In the NN + EA group, the relative density of NF$^+$ axons was also obviously higher than that in the GS and GS + EA groups, as well as that at the area rostral to the injury/graft site in the NN group (Figures S4).

Improvement of Locomotor Function

As a widely used clinical electrophysiological evaluation, the latency and amplitude of evoked potentials were used as major parameters to reflect the nerve conduction velocity and the number of nerve fibers, respectively. In the Sham group, cortical motor evoked potential (CMEP) and somatosensory evoked potential (SSEP) had a large response amplitude and shortened latency (Figures 6A and S6A). In the GS group, rats showed weak CMEP and SSEP signals, but the GS + EA and NN groups showed greatly improved CMEPs and SSEPs (Figures 6A–6C and S6). Wonderfully, NN + EA treatment could further shorten the latency and increase the amplitudes of CMEPs and SSEPs compared with other treatments (Figures 6C and S6).

The hindlimbs of the rats were completely paralyzed following T10 spinal cord transection. From 4 weeks after SCI, hindlimb locomotor performance was improved gradually in all groups. At the end of the eighth week, the Basso, Beattie, and Bresnahan (BBB) score of the NN + EA (7.33 ± 0.65) group was significantly higher than that of the GS (3.33 ± 0.49), GS + EA (4.92 ± 0.67), and NN (5.67 ± 0.72) groups (Figure 6D). At 8 weeks after SCI, the results of the 45° inclined grid climb test showed that all 10 NN + EA treated animals (100%) responded with at least one hindlimb to light touch (contact placing) and joint bending (proprioceptive) stimuli (Figures 6E and 6F, Video S1). It was significantly higher than the percentage of contact placing or proprioceptive responses in the GS (20% or 30%), GS + EA (40% or 50%), and NN (40% or 60%) groups. In the NN + EA group, the contact placing was symmetrical in six rats and proprioceptive response in eight rats, which was higher than that in the GS group. Although the sensorimotor reflexes in the GS + EA and NN groups were improved, there was no statistical difference compared with the GS group (Figure 6E).

Detecting NT-3 Level and TRKC/AKT Molecule Activities in the Injured Spinal Cord

Here, we explored whether EA could maintain NT-3 at a higher level in the injury/graft site and sustain the survival, neuronal differentiation, and synaptic formation of grafted NN by the NT-3/TRKC/AKT signal pathway. The results of ELISA and western blot showed that EA indeed could increase NT-3 level (Figure S4) and augment expression of p-TRKC in the injury/graft site at 8 weeks after SCI in the GS + EA and NN + EA groups (Figures 7A and 7B). Moreover, p-TRKC and p-AKT expression levels in the NN + EA group were higher than in other groups (Figure 7B). Furthermore, the percentages of p-TRKC$^+$GFP$^+$ and p-AKT$^+$GFP$^+$ cells in the NN + EA (24.86% ± 2.57% and 33.60% ± 4.47%) group were increased compared with the NN (7.40% ± 1.77% and 9.95% ± 2.15%) group (Figures 7C and 7D). The results suggest that NN + EA can increase NT-3 level and activate the TRKC/AKT signaling pathway to promote the survival, neuronal differentiation, and synaptic formation of grafted cells in the injury/graft site of spinal cord.

DISCUSSION

Our previous study found that EA treatment can improve the microenvironment of the injury site of spinal cord and promote the migration of grafted stem cells (Chen et al., 2008; Ding et al., 2009). However, the donor NSCs showed a low survival rate. Therefore, this study was extended to investigate whether cell survival and synaptic transmission within NT-3 and TRKC gene-overexpressing NN grafted into transected spinal cord could be promoted by EA through improving the microenvironment at 8 weeks after SCI. The major finding in the present study is that EA markedly enhanced the survival and synaptic integration of grafted NN with the host spinal neural network by increasing NT-3 level and activating the NT-3/TRKC/AKT signaling pathway in the injured spinal cord tissue.

Figure 4. PRV Retrograde Tracing of Transplanted NSC-Derived Neurons in the Injury/Graft Site of Spinal Cord
(A) A schematic diagram showing injection of PRV as a neuroanatomical tracer into the sciatic nerve. This resulted in transsynaptic and retrograde labeling of the grafted NN, thus demonstrating it as neuronal relays that can rebuild the synaptic integration with host neural circuits.
(B) Representative images showing that the MAP2$^+$ (purple) host or NSC-derived neurons (arrowheads) were retrogradely labeled by PRV (red) in the rostral and caudal areas to and in the injury/graft site of spinal cord in the GS (B1–B6), GS + EA (B7–B12), NN (B13–B18), and NN + EA (B19–B24) groups.
(C) Bar chart showing the number of PRV-labeled neurons in the T9, T10, and T11 areas in 4 groups (n = 3/group; one-way ANOVA with LSD t, *p < 0.05 indicates significant difference from GS group; #p < 0.05 indicates significant difference from GS + EA; &p < 0.05 indicates significant difference from NN group).
Scale bars: 20 μm in (B1)–(B14), (B17)–(B20), (B23), and (B24); 10 μm in (B15), (B16), (B21), and (B22).
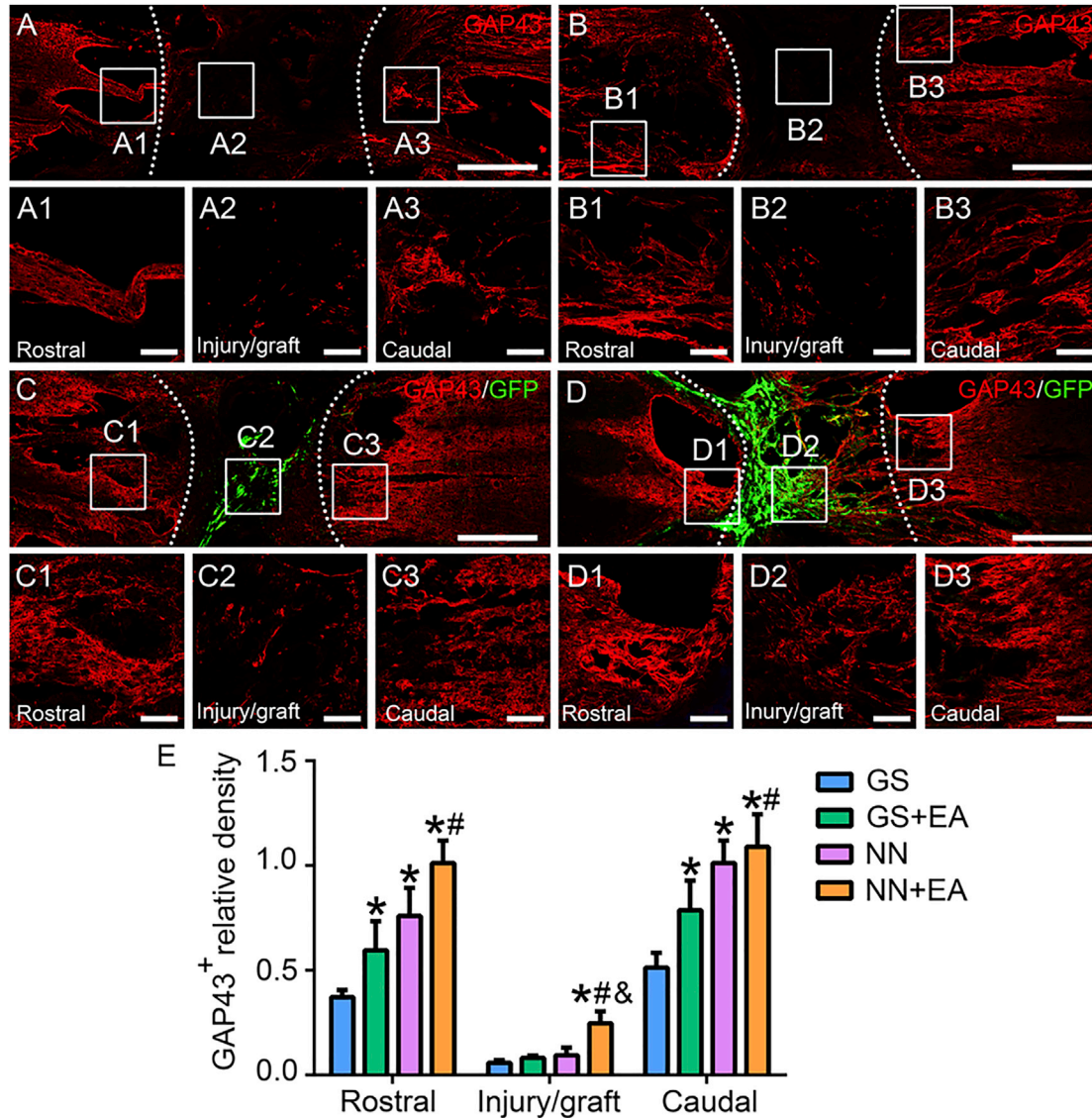
Figure 5. Assessment of GAP43$^+$ Axons in the Injury/Graft Site of Spinal Cord

(A–D) Representative images showing GAP43$^+$ axons in the (A) GS, (B) GS + EA, (C) NN, and (D) NN + EA groups. The dashed curves outline the interface of graft and host. The enlarged images from the rostral and caudal areas and the injury/graft site of spinal cord are shown in (A1–A3), (B1–B3), (C1–C3), and (D1–D3).

(E) Bar charts showing GAP43$^+$ axon relative density in the rostral and caudal areas and the injury/graft site in 4 groups (n = 5/group; one-way ANOVA with LSD t, *p < 0.05 indicates significant difference from the GS group; #p < 0.05 indicates significant difference from the GS + EA group; &p < 0.05 indicates significant difference from the NN group).

Scale bars: 1 mm in (A–D); 100 μm in (A1)–(A3), (B1)–(B3), (C1)–(C3), and (D1)–(D3).

Here, we replaced the PLGA scaffold with a cylindrical GS scaffold for the construction of a 3D neural network scaffold because GS has a chemical composition similar to that of collagen, yet lacks antigenicity (Gamez Sazo et al., 2012; Niu et al., 2014). *In vitro*, the NN had higher expression of neuronal marker MAP2, pre-synaptic marker SYN, and post-synaptic marker PSD95 with typical synaptic structure in the NT-3 NSC + TRKC NSC group, along with

APs and higher frequency of mEPSCs compared with other groups. These results confirmed that overexpression of NT-3 and TRKC could enhance the functional maturation of the NSC-derived neurons. These findings are supported by the previous studies, which have demonstrated that NT-3 binding to its receptor TRKC can initiate synaptic modifications through the Rap1-MAPK, CaMKIV-CREB, and PI3K/AKT signal pathways (Je et al., 2006; Lai et al.,
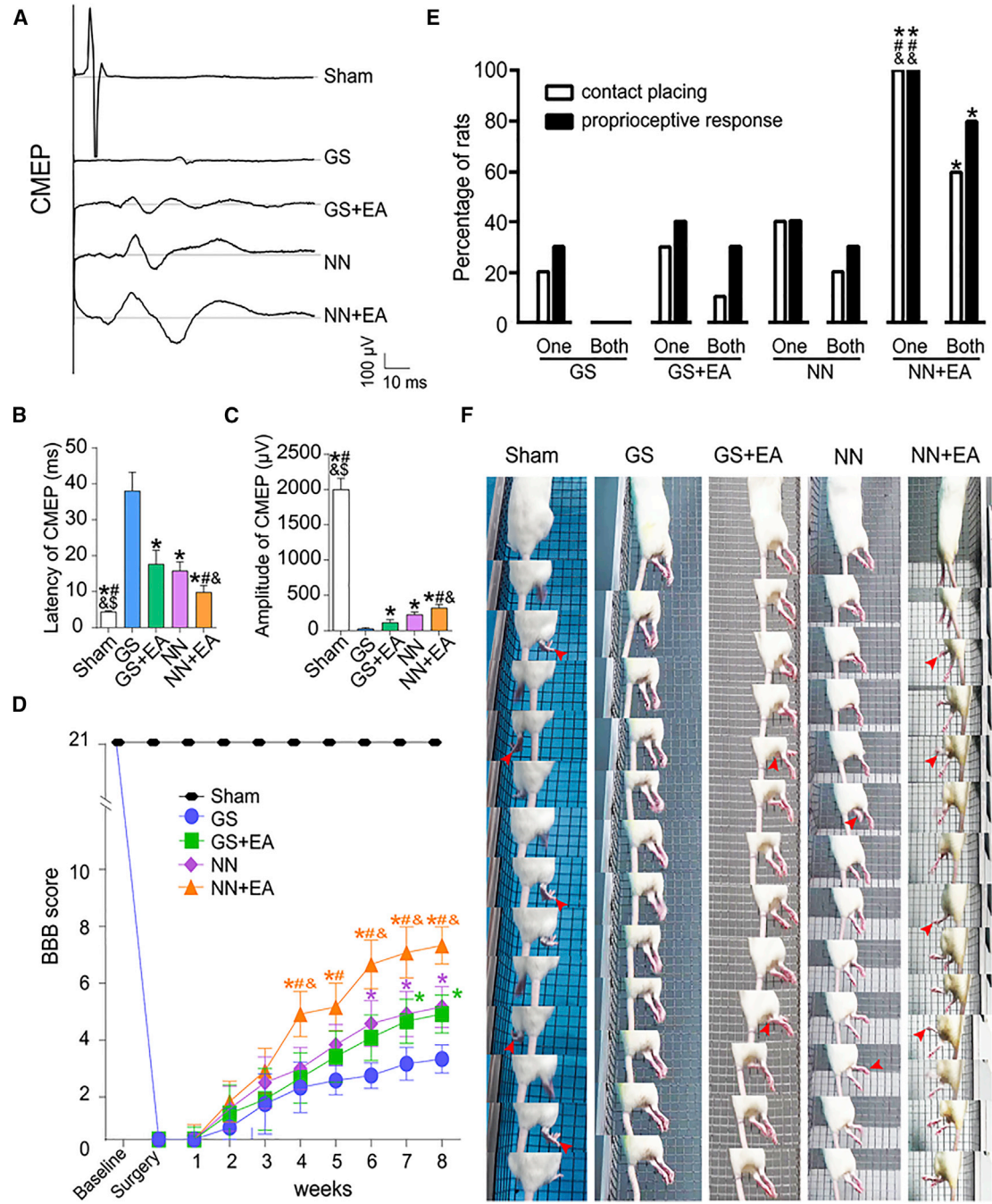
Figure 6. Outcomes of Electrophysiology, BBB Locomotion Assessment, and Grid Climb Test

(A) CMEPs were obtained by electrophysiological analysis in the GS, GS + EA, NN, and NN + EA groups.

(B and C) Bar charts showing the (B) latency and (C) amplitude of CMEPs (n = 5/group; one-way ANOVA with LSD t).

(D) Graph of BBB score of the hindlimb locomotor function in 5 groups (n = 10/group; one-way ANOVA with LSD t).

(E) Bar charts showing the percentage of rats that recovered two sensorimotor reflexes with one hindlimb or two hindlimbs in 45° inclined grid climb test (n = 10/group; Fisher's exact test).

(F) Serial pictures of movement of the rats' feet (arrowheads) while crawling upward from bottom.

$*p < 0.05$ indicates significant difference from the GS group; [#]$p < 0.05$ indicates significant difference from the GS + EA group; [&]$p < 0.05$ indicates significant difference from the NN group; [$]$p < 0.05$ indicates significant difference from the NN + EA group.
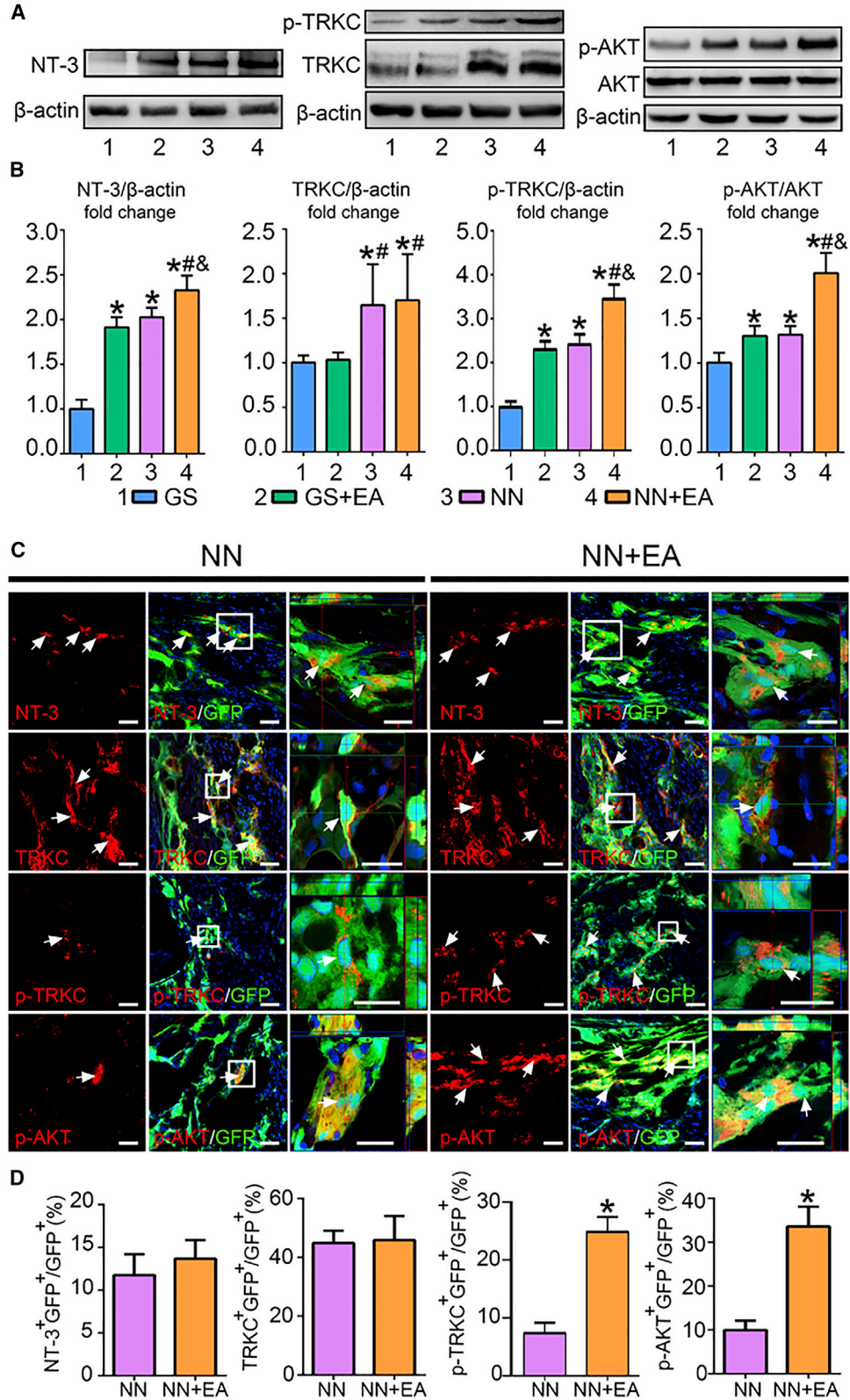
(legend on next page)

2016). In addition, a recent study has reported that NT-3 is required for TRKC-dependent pre-synaptic differentiation through increased binding of dimerized TRKC with pre-synaptic protein tyrosine phosphatase σ (Han et al., 2016a). These data indicate that the co-cultured NT-3 NSCs and TRKC NSCs in a 3D GS scaffold are able to create a tissue-engineered neuronal network by forming synaptic connections among the NSC-derived neurons.

In severe SCI, with the lack of essential neurotrophic factors coupled with unfavorable microenvironment, only a small fraction of NSC-derived neurons in a grafted neural network can survive and differentiate into neurons in the injury/graft site of the spinal cord (Lin et al., 2016). It has been reported that transplantation of fibrin matrices containing NSCs with various growth factors dramatically enhanced graft survival in an SCI model, and graft-derived neurons thus obtained long-distance axonal growth and partially restored the disrupted neural circuits (Lu et al., 2012). However, the use of neurotrophic factors is hindered due to the short half-life in the systemic circulation. To avoid these undesirable outcomes, we attempted to use EA to enhance the survival and synaptic integration of the grafted NN with the host spinal circuit of the transected spinal cord. EA treatment has been widely used and is known for its benefits in restoration, synapse formation, and neural rehabilitation after SCI, which may be attributed to its enhancement of neurotrophic factor secretion, anti-oxidation, anti-inflammation, and anti-apoptosis (Jiang et al., 2014; Renfu et al., 2014; Zhang et al., 2017). EA is also considered as an electrical stimulation model for specific acupoints. There is increasing evidence that low-frequency electrical stimulation can inhibit neuronal apoptosis and promote neural regeneration *in vitro* and *in vivo* (Greenebaum, 2015; Hamid and Hayek, 2008; Han et al., 2016b).

The present results from GFP⁺ cell counting and GFP western blot demonstrated that EA could increase grafted cell survival, and the findings of IF, IEM, and electrophysiology also indicated that grafted cells differentiating into neurons (including excitatory and inhibitory neurons) could form synapses and be activated during signal transmission, and the end result is that excitatory signaling plays a dominant role. As Steward concluded, excitatory neurons act as neuronal relays and are a key component in transmitting signals from the brain to the spinal cord (Bonner and Steward, 2015). Although specific molecular mechanisms remain to be elucidated, the present study has shown that EA can promote the long-term persistent expression of endogenous NT-3 along with the activation of p-TRKC and p-AKT in the injury/graft site. Activated AKT (p-AKT) is involved in the regulation of several important cellular processes in neurons, including survival, differentiation, and metabolism (Dudek et al., 1997; Sinor and Lillien, 2004). We have reported previously that the PI3K/AKT/mTOR and PI3K/AKT/CREB pathways, but not the αCAMKII/CREB pathway, control the formation of synapses for NSC-derived neurons in 3D culture (Lai et al., 2016). Here we have added that NN implants combined with EA could activate the NT-3/TRKC/AKT signal pathway in the injury/graft site. Taken together, the results indicate that EA is advantageous to the survival, neuronal differentiation, and synaptic maintenance of grafted NN, which could partly be attributed to the increased NT-3.

Most importantly, our results from PRV retrograde tracing, IEM, and electrophysiological detection revealed that EA can reinforce the synaptic integration of donor neurons in the NN with host spinal neural circuits, and facilitate spinal descending or ascending nerve conduction 8 weeks post-transplantation. PRV, a retrograde transsynaptic marker (Card et al., 1990), was used to analyze functional synaptic connections between the grafted NN and the host spinal cord. The spatial-temporal progression of PRV infection in the CNS after the peripheral injection has been well documented (Bareyre et al., 2004). It was reported that PRV labeling is restricted to the lumbar motor neurons at 2 days post-injection, while the virus is seen in the cell bodies of interneurons of the cervical spinal cord at 5 days post-injection. However, because of the complete transection of the T10 segments (2-mm segment was removed) in our study, the injury/graft site lacked the large numbers of functional interneurons that would take up and transport PRV from the caudal area to the rostral area of injured spinal cord. This is a possible explanation for the absence of PRV⁺ neurons in control groups in areas rostral to the injury/graft site of spinal cord. Nevertheless, PRV⁺ neurons were observed in the injury/graft site or areas rostral to it in both the NN and the NN + EA groups. Remarkably, in the NN + EA group, the number of PRV⁺

Figure 7. Combination of NN Transplantation and EA Increased NT-3 Level and Activated TRKC/AKT Signaling Pathway
(A and B) (A) Western blot analysis and (B) quantitation of NT-3, TRKC, p-TRKC, and p-AKT protein expression in the injury/graft site of spinal cord at 8 weeks after SCI (n = 5/group). *p < 0.05 indicates significant difference from the GS group; #p < 0.05 indicates significant difference from the GS + EA group; &p < 0.05 indicates significant difference from the NN group by one-way ANOVA followed by LSD t.
(C) Representative images showing the GFP⁺ cells colocalized with NT-3, TRKC, p-TRKC, and p-AKT (yellow, arrows). The boxed areas are shown with their corresponding higher magnification images.
(D) Bar charts showing the percentage of GFP⁺ cells colocalized with NT-3, TRKC, p-TRKC, and p-AKT (n = 5/group).
Student's t test, *p < 0.05 indicates significant difference from the NN group by Student's t test. Scale bars, 20 μm in (C).

neurons in the areas rostral to or in the injury/graft site was more than that in the NN group. A possible explanation for this is that EA treatment may facilitate more synaptic integration of grafted NN with the host neural network of spinal cord. Furthermore, the shorter latency and higher amplitude of CMEPs and SSEPs in the NN + EA group also suggest that EA promotes the donor neurons from the grafted NN to establish more synaptic connections with the host spinal neurons. In addition, IEM further showed that the grafted GFP^{+} cells could form a synapse-like structure with host neurons in the NN + EA group.

The combinational treatment (NN + EA) also promotes the improvement of hindlimb locomotor and sensory function. It is reasonable to consider that the NN + EA treatment could enhance host axonal regeneration and reconstruction of synaptic connections with grafted NN to restore the disrupted nerve conduction circuits. Another consideration is the higher concentrations of neurotrophic factors that can make a significant contribution to axonal regeneration of injured spinal cord. EA is known to elicit secretion of a large amount of neurotrophic factors that can provide protective or pro-regenerative effects to host spinal cord tissue (Chen et al., 2007; Wu et al., 2015). It is conceivable that the NN + EA treatment would promote regeneration of the descending and ascending axons into the injury/graft site and rebuilding of the synaptic connections with the grafted NN to restore host spinal neural circuits, and finally enhance the improvement of spinal cord nerve conduction and the locomotor and sensorimotor reflex of hindlimbs. In addition, EA enhanced the long-term survival, differentiation, and synaptogenesis of grafted NSC-derived neurons, which could in turn amplify the role of EA in increasing neural conduction velocity by forming neuronal relays (Adler et al., 2017; Ding et al., 2015, 2009). Interestingly, a recent study reported that injured adult axons retain the ability to regenerate into appropriate targets and avoid inappropriate targets of grafted neural progenitors (Dulin et al., 2018). These results suggest that the combination therapy can not only provide eventually a greater number of neurons, but also lead to activating the neuronal intrinsic programs that support axonal growth and formation of synaptic connections. AKT activation in grafted NN induced by EA treatment as demonstrated in this study may be one example of this, because AKT activation is not only necessary for the survival and synaptic development of NSC-derived neurons, but also essential for axonal regeneration and plasticity (Al-Ali et al., 2017; Harrison et al., 2016). Therefore, increased endogenous NT-3 level induced by EA may also partly endow the host axons or propriospinal neurons with higher intrinsic capability of integration with the grafted NSC-derived neurons.

In conclusion, the present results have demonstrated that EA treatment can reinforce the survival, neuronal differentiation, and synaptic connections of donor neurons in NN scaffolds by increasing NT-3 levels and activating the NT-3/TRKC/AKT pathway. Moreover, the combinational therapy of grafted NN and EA fosters host axonal regeneration into the injury/graft site to rebuild the synaptic connections with the grafted NN and partly restore spinal neural circuits, and finally improves the nerve conduction of the spinal cord as well as the locomotor function of the paralyzed hindlimbs.

EXPERIMENTAL PROCEDURES

Cell Culture and Genetic Modification

NSCs were isolated and cultured as previously described from GFP transgenic SD neonatal rats (Osaka University, Osaka, Japan; Lai et al., 2013). The second-passage NSCs were transfected by recombinant adenovirus containing the NT-3 gene (Ad-NT-3) or TRKC gene (Ad-TRKC).

Preparation of a Gelatin Sponge Scaffold and Genetically Modified NSCs Seeded in the GS

A commercial gelatin sponge (Nanjing Jinling Co., Nanjing, China) with a pore size of 200–600 μm and a PLGA cylindrical tube 3 mm in diameter and 2 mm in length were used (Figure 1B) for cell transplantation. The PLGA tube was filled with the gelatin sponge under sterile conditions as previously described (Zeng et al., 2011) to form a cylindrical-shaped GS following seeding of cells. GSs were first pre-wet and then excess liquid was siphoned off. A cell suspension was dropped onto the surface of the GS and a sterilizing filter was placed at its bottom to gently suck cells into the pores. Four groups of cells *in vitro* were designed in the present study. These included the NSCs, NT-3 NSCs (NT-3 gene overexpressed in NSCs), TRKC NSCs (TRKC gene overexpressed in NSCs), and NT-3 NSCs + TRKC NSCs (NT-3 NSCs mixed with TRKC NSCs in a 1:1 ratio) groups. A total of 1×10^6 cells were seeded into each GS. The scaffolds were then incubated for 14 days in Neurobasal Medium (Gibco, CA, USA) with 2% B27 supplement (Gibco, CA, USA). The culture medium was replaced every 2 days.

Immunofluorescence Staining

Specific proteins were detected by IF staining as reported previously (Qiu et al., 2015). Briefly, the post-fixed scaffolds and spinal cord were sectioned at 20 μm thickness with a cryostat. The sections were rinsed with 0.01 M phosphate-buffered saline (PBS) three times, blocked with 10% goat serum for 30 min, and incubated with primary antibodies containing 0.3% Triton X-100 overnight at 4°C. After being rinsed in PBS, the sections were incubated with secondary antibodies and examined under a fluorescence microscope. A summary of the antibodies used is provided in Table S1.

Spinal Cord Transection and Grouping

To prepare a complete SCI model, adult female SD rats (7–8 weeks old, 220–250 g, supplied by the Experimental Animal Center

of Sun Yat-sen University, China) were used. All experimental protocols and animal handling procedures were approved by the Animal Care and Use Committee of Sun Yat-sen University and were consistent with the National Institutes of Health *Guide for the Care and Use of Laboratory Animals*. Three days before surgery, animals were given cyclosporin A by subcutaneous injection (1 mg/100 g/rat). The animals were anesthetized with 1% pentobarbital sodium (40 mg/kg, intraperitoneally). A laminectomy was carried out to expose the T10 spinal segments and completely transect the spinal cord, and then a 2-mm T10 segment of spinal cord was removed. The rats underwent transplantation with the GS or the NN constructed with overexpressing NT-3 NSCs or overexpressing TRKC NSCs. Then, the animals were divided into four groups (n = 10 for each group): the GS group received only GS without cells, the GS + EA group received the GS with EA treatment, the NN group received only the NN graft, and the NN + EA group received the NN graft with EA treatment. After the surgical incisions were sutured, the rats received post-operative care, including intramuscular injection of penicillin (50,000 U/kg/day) for 3 days and manual emiction two times daily until their automatic micturition function was reestablished. Cyclosporin A (1 mg/100 g) was administered once daily for 2 months.

Electroacupuncture

EA stimulation was applied at two pairs of GV acupoints, (1) GV9 (Zhiyang) and GV6 (Jizhong) and (2) GV2 (Yaoshu) and GV1 (Changqiang), as described previously (Ding et al., 2009). EA treatment is a pattern of sparse to dense wave alternating stimulation pulses. The pattern of stimulus frequency and duration is repeats of 2 Hz for 2.85 s and 60 Hz for 1.05 s as a repeating cycle. During the process of EA, the current intensity in the animal's body between the pair of acupoints across the grafts was tested, and the current intensity cycle was ∼5 μA. Each EA treatment lasted for 20 min. EA treatment was given every other day for 8 weeks, starting from the third day post-surgery.

Assessment of Locomotor Performance

Hindlimb function of the rats was assessed weekly after surgery, using the BBB open-field locomotor test (Basso et al., 1995) and inclined-grid climbing test (Ramon-Cueto et al., 2000). The former quantitatively evaluates voluntary movement and body weight support. The latter assesses the percentage of rats that recovered the contact placing and proprioceptive responses of hindlimbs. All behavior tests were videotaped, and two investigators blind to the different experimental treatments evaluated the functional outcome of each animal by reviewing the videotapes. Each foot was assessed independently, and a positive score for each hindlimb was given only if there were at least two clear responses during at least two consecutive sessions.

Electrophysiological Analysis

At the end of the experiment, evoked potentials were recorded as described previously to assess functional status of motor and sensory axonal conduction (Guo et al., 2007; Wang et al., 2011). Basically, following general anesthesia and exposure of the sensorimotor cortex (SMC) and sciatic nerves, the electrodes (NeuroExam M-800 Data Acquisition Analysis System, MEDCOM,

Zhuhai, China) were connected to the SMC and sciatic nerve, respectively. When detecting the CMEP, the stimulating electrodes (active silver midline epidural electrodes) were placed in the SMC (located 2 mm lateral to midline and 2 mm caudal to bregma) and the recording electrodes were connected with the sciatic nerve according to our previous study (Lai et al., 2018). Fifty response waveforms of CMEP and SSEP were collected and averaged for each rat with stimulation of the right and left sensorimotor cortex and sciatic nerve, respectively. The averages of amplitude and latency of recorded CMEP and SSEP were analyzed.

Statistical Analysis

All statistical analyses were performed using the statistical software SPSS 22.0. Data were expressed as mean ± standard deviation. The data were analyzed using one-way ANOVA with least significant difference test applied. When two groups were compared, Student's t test or Fisher's exact test was used. A statistically significant difference was accepted at $p < 0.05$.

SUPPLEMENTAL INFORMATION

Supplemental Information includes Supplemental Experimental Procedures, six figures, one table, and one video and can be found with this article online at https://doi.org/10.1016/j.stemcr.2018.12.015.

REFERENCES

Adler, A.F., Lee-Kubli, C., Kumamaru, H., Kadoya, K., and Tuszynski, M.H. (2017). Comprehensive monosynaptic rabies virus MAP of host connectivity with neural progenitor grafts after spinal cord injury. Stem Cell Reports 8, 1525–1533.

Agbay, A., Edgar, J.M., Robinson, M., Styan, T., Wilson, K., Schroll, J., Ko, J., Khadem Mohtaram, N., Jun, M.B., and Willerth, S.M. (2016). Biomaterial strategies for delivering stem cells as a treatment for spinal cord injury. Cells Tissues Organs 202, 42–51.

Al-Ali, H., Ding, Y., Slepak, T., and Wu, W. (2017). The mTOR substrate S6 kinase 1 (S6K1) is a negative regulator of axon regeneration and a potential drug target for central nervous system injury. J. Neurosci. 37, 7079–7095.

Bareyre, F.M., Kerschensteiner, M., Raineteau, O., Mettenleiter, T.C., Weinmann, O., and Schwab, M.E. (2004). The injured spinal cord spontaneously forms a new intraspinal circuit in adult rats. Nat. Neurosci. 7, 269–277.

Basso, D.M., Beattie, M.S., and Bresnahan, J.C. (1995). A sensitive and reliable locomotor rating scale for open field testing in rats. J. Neurotrauma 12, 1–21.

Bonner, J.F., and Steward, O. (2015). Repair of spinal cord injury with neuronal relays: from fetal grafts to neural stem cells. Brain Res. 1619, 115–123.

Bregman, B.S., Coumans, J.V., Dai, H.N., Kuhn, P.L., Lynskey, J., McAtee, M., and Sandhu, F. (2002). Transplants and neurotrophic factors increase regeneration and recovery of function after spinal cord injury. Prog. Brain Res. 137, 257–273.

Card, J.P., Rinaman, L., Schwaber, J.S., Miselis, R.R., Whealy, M.E., Robbins, A.K., and Enquist, L.W. (1990). Neurotropic properties of pseudorabies virus: uptake and transneuronal passage in the rat central nervous system. J. Neurosci. 10, 1974–1994.

Chao, M.V. (2003). Neurotrophins and their receptors: a convergence point for many signalling pathways. Nat. Rev. Neurosci. 4, 299–309.

Chen, J., Qi, J.G., Zhang, W., Zhou, X., Meng, Q.S., Zhang, W.M., Wang, X.Y., and Wang, T.H. (2007). Electro-acupuncture induced NGF, BDNF and NT-3 expression in spared L6 dorsal root ganglion in cats subjected to removal of adjacent ganglia. Neurosci. Res. 59, 399–405.

Chen, X.M., Xu, J., Song, J.G., Zheng, B.J., and Wang, X.R. (2015). Electroacupuncture inhibits excessive interferon-gamma evoked up-regulation of P2X4 receptor in spinal microglia in a CCI rat model for neuropathic pain. Br. J. Anaesth. 114, 150–157.

Chen, Y.Y., Zhang, W., Chen, Y.L., Chen, S.J., Dong, H., and Zeng, Y.S. (2008). Electro-acupuncture improves survival and migration of transplanted neural stem cells in injured spinal cord in rats. Acupunct. Electrother. Res. 33, 19–31.

Ding, Y., Yan, Q., Ruan, J.W., Zhang, Y.Q., Li, W.J., Zhang, Y.J., Li, Y., Dong, H., and Zeng, Y.S. (2009). Electro-acupuncture promotes survival, differentiation of the bone marrow mesenchymal stem cells as well as functional recovery in the spinal cord-transected rats. BMC Neurosci. 10, 35.

Ding, Y., Zhang, R.Y., He, B., Liu, Z., Zhang, K., Ruan, J.W., Ling, E.A., Wu, J.L., and Zeng, Y.S. (2015). Combination of electroacu-puncture and grafted mesenchymal stem cells overexpressing TrkC improves remyelination and function in demyelinated spinal cord of rats. Sci. Rep. 5, 9133.

Du, B.L., Xiong, Y., Zeng, C.G., He, L.M., Zhang, W., Quan, D.P., Wu, J.L., Li, Y., and Zeng, Y.S. (2011). Transplantation of artificial neural construct partly improved spinal tissue repair and functional recovery in rats with spinal cord transection. Brain Res. 1400, 87–98.

Du, B.L., Zeng, C.G., Zhang, W., Quan, D.P., Ling, E.A., and Zeng, Y.S. (2014). A comparative study of gelatin sponge scaffolds and PLGA scaffolds transplanted to completely transected spinal cord of rat. J. Biomed. Mater. Res. A 102, 1715–1725.

Dudek, H., Datta, S.R., Franke, T.F., Birnbaum, M.J., Yao, R., Cooper, G.M., Segal, R.A., Kaplan, D.R., and Greenberg, M.E. (1997). Regulation of neuronal survival by the serine-threonine protein kinase Akt. Science 275, 661–665.

Dulin, J.N., Adler, A.F., Kumamaru, H., Poplawski, G.H.D., Lee-Kubli, C., Strobl, H., Gibbs, D., Kadoya, K., Fawcett, J.W., Lu, P., and Tuszynski, M.H. (2018). Injured adult motor and sensory axons regenerate into appropriate organotypic domains of neural progenitor grafts. Nat. Commun. 9, 84.

Gamez Sazo, R.E., Maenaka, K., Gu, W., Wood, P.M., and Bunge, M.B. (2012). Fabrication of growth factor- and extracellular matrix-loaded, gelatin-based scaffolds and their biocompatibility with Schwann cells and dorsal root ganglia. Biomaterials 33, 8529–8539.

Greenebaum, B. (2015). Calculated spinal cord electric fields and current densities for possible neurite regrowth from quasi-DC electrical stimulation. Bioelectromagnetics 36, 564–575.

Guo, J.S., Zeng, Y.S., Li, H.B., Huang, W.L., Liu, R.Y., Li, X.B., Ding, Y., Wu, L.Z., and Cai, D.Z. (2007). Cotransplant of neural stem cells and NT-3 gene modified Schwann cells promote the recovery of transected spinal cord injury. Spinal Cord 45, 15–24.

Hamid, S., and Hayek, R. (2008). Role of electrical stimulation for rehabilitation and regeneration after spinal cord injury: an overview. Eur. Spine J. 17, 1256–1269.

Han, K.A., Woo, D., Kim, S., Choii, G., Jeon, S., Won, S.Y., Kim, H.M., Heo, W.D., Um, J.W., and Ko, J. (2016a). Neurotrophin-3 regulates synapse development by modulating TrkC-PTPsigma synaptic adhesion and intracellular signaling pathways. J. Neurosci. 36, 4816–4831.

Han, S., Kim, D., Kim, H., Park, J.W., and Youn, I. (2016b). Electrical stimulation inhibits cytosine arabinoside-induced neuronal death by preventing apoptosis in dorsal root ganglion neurons. Neuroreport 27, 1217–1224.

Harrison, B.J., Venkat, G., Lamb, J.L., Hutson, T.H., Drury, C., Rau, K.K., Bunge, M.B., Mendell, L.M., Gage, F.H., Johnson, R.D., et al. (2016). The adaptor protein CD2AP is a coordinator of neurotrophin signaling-mediated axon arbor plasticity. J. Neurosci. 36, 4259–4275.

Hofstoetter, U.S., Freundl, B., Binder, H., and Minassian, K. (2018). Common neural structures activated by epidural and transcutaneous lumbar spinal cord stimulation: Elicitation of posterior root-muscle reflexes. PLoS One 13, e0192013.

Je, H.S., Yang, F., Zhou, J., and Lu, B. (2006). Neurotrophin 3 induces structural and functional modification of synapses through distinct molecular mechanisms. J. Cell Biol. *175*, 1029–1042.

Jiang, S.H., Tu, W.Z., Zou, E.M., Hu, J., Wang, S., Li, J.R., Wang, W.S., He, R., Cheng, R.D., and Liao, W.J. (2014). Neuroprotective effects of different modalities of acupuncture on traumatic spinal cord injury in rats. Evid. Based Complement. Alternat. Med. *2014*, 431580.

Kumar, S., Dey, S., and Jain, S. (2017). Extremely low-frequency electromagnetic fields: a possible non-invasive therapeutic tool for spinal cord injury rehabilitation. Electromagn. Biol. Med. *36*, 88–101.

Lai, B.Q., Che, M.T., Du, B.L., Zeng, X., Ma, Y.H., Feng, B., Qiu, X.C., Zhang, K., Liu, S., Shen, H.Y., et al. (2016). Transplantation of tissue engineering neural network and formation of neuronal relay into the transected rat spinal cord. Biomaterials *109*, 40–54.

Lai, B.Q., Feng, B., Che, M.T., Wang, L.J., Cai, S., Huang, M.Y., Gu, H.Y., Jiang, B., Ling, E.A., Li, M., et al. (2018). A modular assembly of spinal cord-like tissue allows targeted tissue repair in the transected spinal cord. Adv. Sci. (Weinh). *5*, 1800261.

Lai, B.Q., Wang, J.M., Duan, J.J., Chen, Y.F., Gu, H.Y., Ling, E.A., Wu, J.L., and Zeng, Y.S. (2013). The integration of NSC-derived and host neural networks after rat spinal cord transection. Biomaterials *34*, 2888–2901.

Lin, X.Y., Lai, B.Q., Zeng, X., Che, M.T., Ling, E.A., Wu, W., and Zeng, Y.S. (2016). Cell transplantation and neuroengineering approach for spinal cord injury treatment: a summary of current laboratory findings and review of literature. Cell Transplant. *25*, 1425–1438.

Lu, P., Wang, Y., Graham, L., McHale, K., Gao, M., Wu, D., Brock, J., Blesch, A., Rosenzweig, E.S., Havton, L.A., et al. (2012). Long-distance growth and connectivity of neural stem cells after severe spinal cord injury. Cell *150*, 1264–1273.

Niu, G., Choi, J.S., Wang, Z., Skardal, A., Giegengack, M., and Soker, S. (2014). Heparin-modified gelatin scaffolds for human corneal endothelial cell transplantation. Biomaterials *35*, 4005–4014.

Poo, M.M. (2001). Neurotrophins as synaptic modulators. Nat. Rev. Neurosci. *2*, 24–32.

Qiu, X.C., Jin, H., Zhang, R.Y., Ding, Y., Zeng, X., Lai, B.Q., Ling, E.A., Wu, J.L., and Zeng, Y.S. (2015). Donor mesenchymal stem cell-derived neural-like cells transdifferentiate into myelin-forming cells and promote axon regeneration in rat spinal cord transection. Stem Cell. Res. Ther. *6*, 105.

Ramon-Cueto, A., Cordero, M.I., Santos-Benito, F.F., and Avila, J. (2000). Functional recovery of paraplegic rats and motor axon regeneration in their spinal cords by olfactory ensheathing glia. Neuron *25*, 425–435.

Renfu, Q., Rongliang, C., Mengxuan, D., Liang, Z., Jinwei, X., Zongbao, Y., and Disheng, Y. (2014). Anti-apoptotic signal transduction mechanism of electroacupuncture in acute spinal cord injury. Acupunct. Med. *32*, 463–471.

Sinor, A.D., and Lillien, L. (2004). Akt-1 expression level regulates CNS precursors. J. Neurosci. *24*, 8531–8541.

Wang, J.M., Zeng, Y.S., Liu, R.Y., Huang, W.L., Xiong, Y., Wang, Y.H., Chen, S.J., and Teng, Y.D. (2007). Recombinant adenovirus vector-mediated functional expression of neurotropin-3 receptor (TrkC) in neural stem cells. Exp. Neurol. *203*, 123–127.

Wang, J.M., Zeng, Y.S., Wu, J.L., Li, Y., and Teng, Y.D. (2011). Cograft of neural stem cells and Schwann cells overexpressing TrkC and neurotrophin-3 respectively after rat spinal cord transection. Biomaterials *32*, 7454–7468.

Wu, M.F., Zhang, S.Q., Liu, J.B., Li, Y., Zhu, Q.S., and Gu, R. (2015). Neuroprotective effects of electroacupuncture on early- and late-stage spinal cord injury. Neural Regen. Res. *10*, 1628–1634.

Xiong, Y., Zeng, Y.S., Zeng, C.G., Du, B.L., He, L.M., Quan, D.P., Zhang, W., Wang, J.M., Wu, J.L., Li, Y., and Li, J. (2009). Synaptic transmission of neural stem cells seeded in 3-dimensional PLGA scaffolds. Biomaterials *30*, 3711–3722.

Yao, L., and Li, Y. (2016). The role of direct current electric field-guided stem cell migration in neural regeneration. Stem Cell Rev. *12*, 365–375.

Yousefifard, M., Rahimi-Movaghar, V., Nasirinezhad, F., Baikpour, M., Safari, S., Saadat, S., Moghadas Jafari, A., Asady, H., Razavi Tousi, S.M.T., and Hosseini, M. (2016). Neural stem/progenitor cell transplantation for spinal cord injury treatment; a systematic review and meta-analysis. Neuroscience *322*, 377–397.

Zeng, X., Zeng, Y.S., Ma, Y.H., Lu, L.Y., Du, B.L., Zhang, W., Li, Y., and Chan, W.Y. (2011). Bone marrow mesenchymal stem cells in a three-dimensional gelatin sponge scaffold attenuate inflammation, promote angiogenesis, and reduce cavity formation in experimental spinal cord injury. Cell Transplant. *20*, 1881–1899.

Zhang, Y.T., Jin, H., Wang, J.H., Wen, L.Y., Yang, Y., Ruan, J.W., Zhang, S.X., Ling, E.A., and Ding, Y. (2017). Tail nerve electrical stimulation and electro-acupuncture can protect spinal motor neurons and alleviate muscle atrophy after spinal cord transection in rats. Neural Plast. *2017*, 7351238.